MANEUVER RECONSTRUCTION, TRACKING SCHEDULING, AND BIAS ESTIMATION IN THE NEAR RECTILINEAR HALO ORBIT (NRHO)

Clark P. Newman,[*] and Diane C. Davis[†]

NASA's Gateway program will build a crew-tended station in an Earth-Moon Near Rectilinear Halo Orbit (NRHO) to support deep space missions to the lunar surface and heliocentric space. The station in the NRHO will be tracked by the Deep Space Network (DSN) with 2-way radiometric tracking data to produce an estimated state that is utilized to target Orbit Maintenance Maneuvers (OMMs). However, the tracking data is corrupted with measurement noise and range bias, which results in state estimation error and OMM execution error. This paper reports on analysis performed to improve the geometry of the tracking data problem with the inclusion of cross-hemispheric partner sites and explores the performance impact of handovers between partner sites and DSN sites. The OMM execution error is estimated directly using a Batch Least Squares (BLS) process, and the range bias estimation is analyzed among both original DSN sites and a combined DSN + partner sites scenario.

INTRODUCTION

Gateway Mission and NRHO

The Gateway will be the first long-term habitable outpost operating beyond Low Earth Orbit (LEO). It will support missions in cislunar space, to the lunar surface, and missions into heliocentric space.[1] The Gateway mission will be in an Earth-Moon southern L2 NRHO with a Lunar synodic ratio of 9:2. This NRHO has a period of approximately 6.5 days and is characterized by long periods of low relative velocity cislunar flight punctuated by brief high-velocity and high-sensitivity perilune passes. The NRHO radius ranges from approximately 3,400 km at perilune to 71,000 km at apolune, and most of the motion is constrained to a plane normal to the Earth-Moon direction.[2] A depiction of the NRHO around the Moon in the foreground with direct transfers to Earth in the background is illustrated in Figure 1. Missions to the NRHO transit via the Outbound trajectory on the right, perform a powered flyby transfer to NRHO, and insert into the NRHO on the right side. Excursions to LLO and the surface originate on the left side approaching Perilune, and transfers from LLO arrive after Perilune passage on the right side. Departure from NRHO is on the left side, again performing a powered flyby to enter the Return trajectory on the left side.

Orbit Determination

The Gateway is assumed to be tracked by the Deep Space Network's (DSN) primary sites of Goldstone, Canberra, and Madrid using an X-band tracking frequency. During uncrewed operations,

---

the vehicle is tracked three times per revolution in 8 hour spans, depicted in Figure 2 on the NRHO in green. Starting after an Orbit Maintenance Maneuver (OMM), there is an 8 hour pre-perilune pass that ends 24 hours before perilune. There is a post-perilune tracking data pass starting 24 hours after perilune for 8 hours, and finally an 8 hour tracking pass that ends 24 hours before OMM execution. While crewed, the Gateway vehicle is tracked continuously, but is also subject to more perturbations from venting and desturation maneuvers. Gateway tracking data consists of 2-way coherent range and range rate. Three-way downlinked range rate data is feasible and investigated as a tracking data scheduling candidate for improved pre-event solutions.
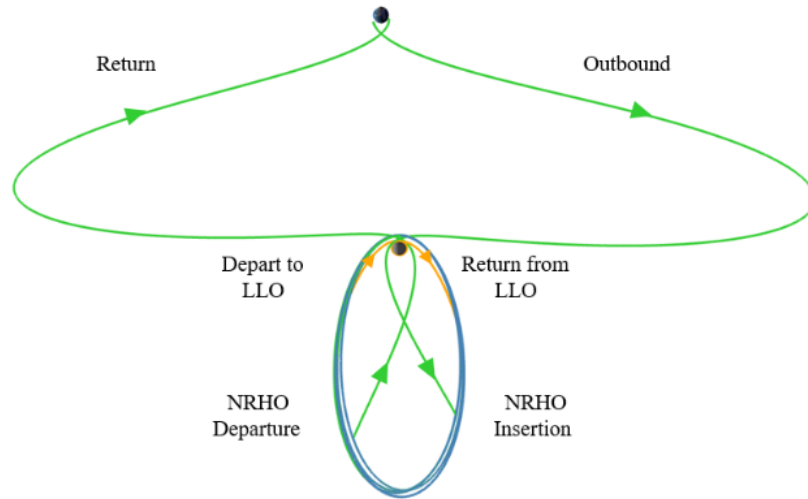

Figure 1: Lunar mission concept: the NRHO in blue, surface excursions in orange, and direct transfers in green, as viewed in the Earth-Moon rotating frame.

Previous and Ongoing Work

As interest in the NRHO has increased, the volume of analysis on navigation in the NRHO has increased, including the first mission to recently arrive on-orbit in the same Southern L2 NRHO, the *Cislunar Autonomous Position System Technology Operations and Navigation Experiment* (CAP-STONE).[3] The basic navigation accuracy expectations from a covariance analysis were first performed by Newman et. al.[4] The feasibility of relative navigation utilizing assets in other lunar orbits was explored by Volle.[5,6] The feasibility and simulated performance of utilizing Global Positioning System (GPS) in the NRHO was explored by Winternitz et. al.[7] Detailed Monte Carlo analysis exploring the impact of tracking schedule, data quality, and error budget were performed by Parrish, Bollinger, et. al. from Advanced Space.[8,9] Navigation analysis considering the operations of a crewed spacecraft were explored by Newman et. al.[10] This paper builds from work completed by the mentioned authors by exploring methods to extract more useful information from the baseline 2-way DSN tracking data.

Additional Sites

Previous work has shown that a tracking data handover across latitudinal hemispheres can significantly reduce estimated state uncertainty as compared to handovers within the same latitudinal hemisphere.[10] As Canberra is the only DSN site in the southern hemisphere, it becomes relatively important compared to Madrid and Goldstone as it is necessarily handed across latitudinal hemi-

spheres at the start of tracking, and at the start of the next site's tracking span.

Additionally, it has been shown that there is difficulty in observing the DSN range bias due to highly parallel measurement paths to the NRHO, and orbital motion in the NRHO being mostly normal to the range direction. This paper investigates whether bias observability improves with cross-latitudinal handovers to/from secondary sites. Observing the range bias can reduce the Mahalonobis distance of solutions which are otherwise aliased by the unobservable range bias into a phenomenon called "filter collapse", where the filtering algorithm has high confidence in an erroneous solution.[11]

To increase the geometric complexity of ground-based tracking data, three partner sites are added to the Gateway network and scheduling rules are adjusted to prefer cross-latitudinal hemispheric handovers between subsequent tracking passes. The additional groundsites are named in lime in the map in Figure 3. Santiago Chile, Hartebeesthoek South Africa, and Usuda Japan are introduced to oppose Goldstone, Madrid, and Canberra, respectively. It is assumed that these additional stations can both accept downlinked 3-way range rate data or two-way coherent range and range rate.

Figure 2: Nominal tracking data arcs visualized on the NRHO for uncrewed operations in lime green.

OMM Reconstruction and Bias Estimation

The Gateway will inhabit a slightly unstable NRHO that must be maintained with small semi-regular OMMs. The OMMs incur errors in thrust scale factor and pointing direction. Nominally, the Square Root Information Filter (SRIF) can follow the post-OMM tracking data pass and adjust the state estimate to reflect the as-executed OMM without specifically characterizing the OMM execution errors. To explicitly estimate OMM thrust scale factor, a Bath Least Squares (BLS) process is executed periodically which considers tracking data before and after the OMM.

The Gateway will be tracked with 2-way tracking per the nominal schedule visualized in Figure 2, and each tracking data pass has a unique, constant, but random range bias. This range bias is minimally observable in the SRIF, which can lead to a condition called "filter collapse" where the state estimate is shifted from the truth with an associated uncertainty that does not correctly capture the true state. This condition is characterized by a high Mahalonobis distance value in position.[11]

To attempt to characterize the tracking data pass range biases, the BLS is again applied periodically to consider multiple tracking data passes at once, to explore if the consideration of multiple passes in the NRHO geometry can increase bias observability of each tracking data pass.
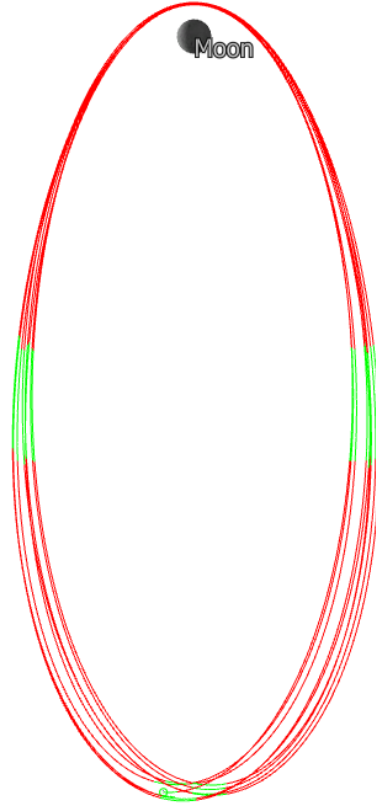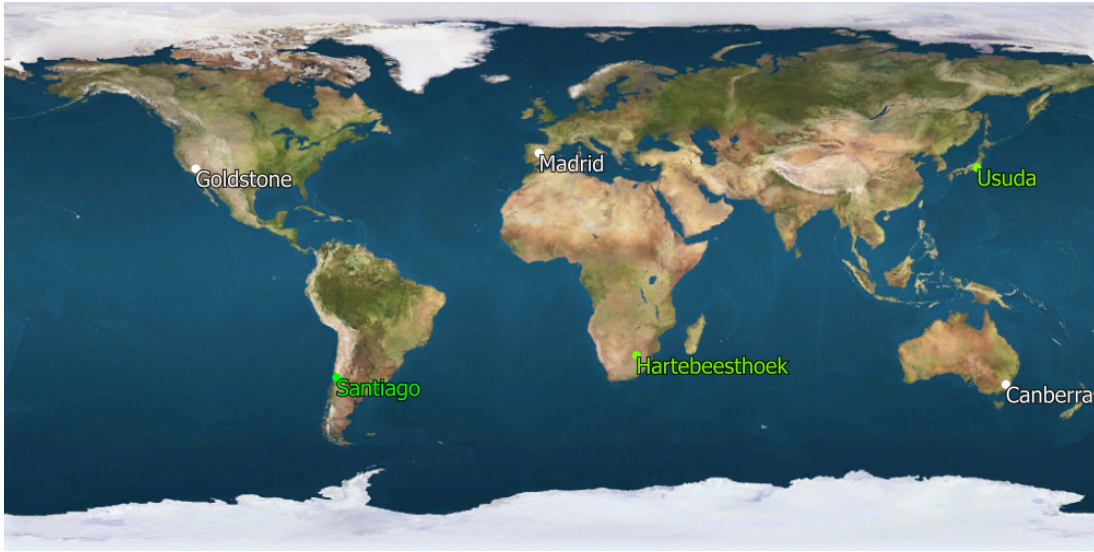
Figure 3: DSN Primary Network (white) and Additional Partner Sites (lime).

SIMULATION

The tracking data simulation, filtering, and BLS execution are all performed in FreeFlyer. The simulation contains a truth spacecraft in the NRHO which executes OMMs once per revolution. Tracking data is simulated between the DSN/partner sites and the truth spacecraft during active data tracking passes. The simulation contains an estimated spacecraft whose state vector is updated by the SRIF by processing the tracking data simulated on the truth spacecraft. The OMM is targeted using the estimated spacecraft state and applied to both the estimated and truth spacecraft. The OMM solution executed on the truth spacecraft contains execution errors such as a pointing error and magnitude error. The OMM solution targets the velocity in the Earth-Moon rotating X direction to match the reference NRHO trajectory on a receding horizon six revolutions from the current state.[12] OMM solutions below a threshold of 3 cm/s are waived to reduce operational burden and perturbations from OMM execution. It has been shown that skipping OMMs below this magnitude does not significantly affect overall propellant use.[12] A diagram illustrating this process appears

In Figure 4, sc_{tru} is tracked with 2-way data from the ground antenna, and that tracking data is processed to update the state of sc_{est} in the Filtering phase. The width of the shaded area represents the uncertainty of the state, which is shown to decrease by processing tracking data through the Filtering phase. Multiple predictive trajectories can be modeled from the final filtered state to include dispersions from random perturbations in the predictive span. The reference spacecraft sc_{ref} trajectory is the target trajectory utilized by the OMM targeting algorithm.[12, 13]

The truth spacecraft is subject to unmodeled perturbations and OMM execution error, while the estimated spacecraft contains a mass modeling error, SRP area error, and is propagated through an adjusted Lunar gravity model of lower degree and order. Error parameters and their values are detailed in Table 1. The tracking data is subject to measurement noise and range bias, the values of which are in Table 2. These errors and perturbations stress the navigation algorithms to accurately update the estimated spacecraft state to closely follow the truth spacecraft state. Unmodeled perturbations include random velocity perturbations from desaturation maneuvers, and for crewed configurations also include CO_2 venting and waste water venting.
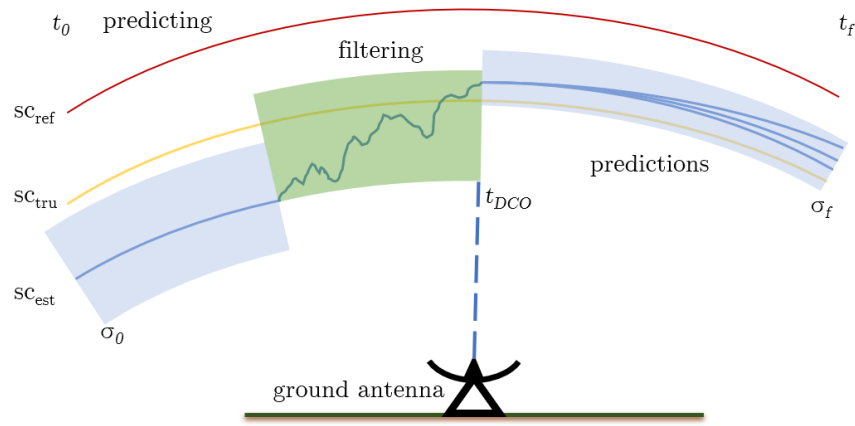
Figure 4: Diagram showing the estimated spacecraft sc$_{tru}$ state updated by tracking data simulated on sc$_{tru}$ in the Filtering phase, and multiple predictions originating from the final filtered state.

Table 1: Simulated Error Sources

Parameter Name	1-σ uncertainty	Notes
Initial Position Error	10 km	
Initial Velocity Error	1 cm/s	
Relative Mass Error	30%	
Relative SRP Area Error	30%	
Desaturation Maneuver ΔV	3.33 mm/s	1, 2
Uncrewed OMM Constant Error	0.47 mm/s	
Uncrewed OMM Magnitude Error	0.5%	
Crewed OMM Magnitude Error	0.5%	
OMM Pointing Error	0.333°	

[1] Desaturation occurs once before OMM execution and three times at perilune for both uncrewed and crewed configurations.
[2] Crewed configurations every 6 hours.

Table 2: Tracking Data Quality Parameters

Parameter	Value (1-σ)
Range Noise (m)	1.0
Range Bias (m)	7.5
Range Rate Noise (mm/s)	0.1

Filtering

The tracking data simulator and SRIF are executed in a tick-tock process as:

1. Step the truth spacecraft forward in time, simulate tracking data as scheduled, execute events as scheduled,
2. Process any tracking data, step the estimated spacecraft forward in time to the truth spacecraft epoch.

The OMM is targeted 24 hours prior to execution at a true anomaly of 200 degrees. As mentioned earlier, the OMM is targeted with the estimated spacecraft state and executed on both the estimated spacecraft and truth spacecraft (with execution errors). Post-OMM tracking data is then processed by the SRIF to update the estimated spacecraft toward the updated trajectory. Perturbations such as desaturation maneuvers are not considered in the filter, but the state estimate is adjusted per the tracking data to consider the resulting velocity perturbations.

Batch Least Squares (BLS)

The SRIF is valuable in maintaining a state estimate that evolves alongside the generation of the simulated tracking data, and is the most intuitive manner to perform OD in general, but considers observations sequentially and in isolation. To consider multiple tracking data passes and estimate the execution error of the maneuver within the data arc, a BLS algorithm is executed at each perilune to process the tracking data collected since the previous perilune. In Figure 5, this process is illustrated in a diagram.
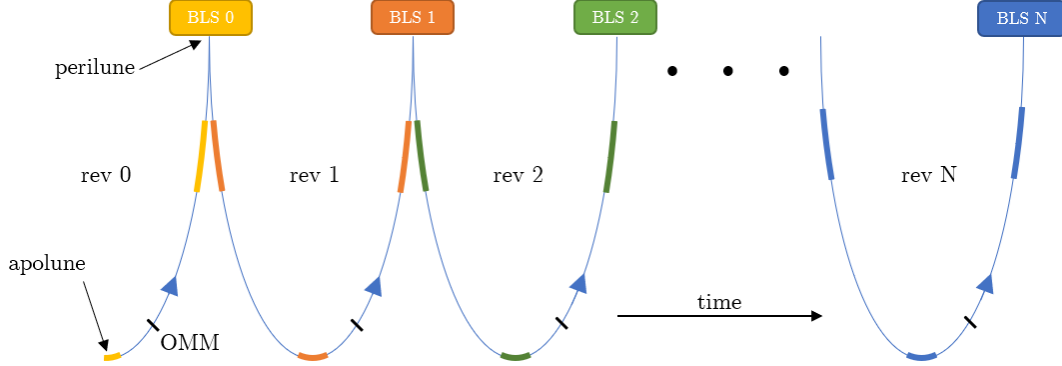

Figure 5: Diagram showing the batching of tracking data for sequential BLS execution, each BLS execution includes the previous revolution's data and OMM.

The simulation starts at apolune in the middle of the pre-OMM tracking data pass, performs the first OMM (or not if the targeted ΔV is below the minimum threshold), and collects the post-OMM tracking data pass observations before arriving at its first perilune passage. The first BLS (labeled "BLS 0" in yellow) is performed with the like-colored data from rev 0 and the first OMM. The initial state estimate for the BLS is derived from the state of sc_{est} from the SRIF. The solution state estimate from the BLS is not fed back into the SRIF, they are separate and contained processes.

The parameters of the BLS are adjusted to investigate its performance in considering OMM scale factor or the tracking data pass range biases. One analysis investigates the feasibility and performance of estimating OMM execution error by directly estimating OMM thrust scale factor in the BLS estimated state vector. Another investigates the feasibility of estimating DSN range bias when considering three passes in each rev together.

Site Selection Logic

The first analysis explores the impact of enforcing variability in the geometry of ground tracking by enforcing handovers across the equator between successive passes. Recall the three partner sites introduced in Figure 3, each paired across the equator from a primary DSN site. The nominal site selection routine would pick the most Eastward site in view to begin a tracking data pass, with no other considerations. The new Hemispheric Handover (HH) selection logic chooses the next site depending on the current or previous site's hemisphere. E.g. if the most recent pass was from the northern hemisphere, the next pass will be forced to be from the southern hemisphere.

Two Monte Carlo analyses were performed on crewed scenarios with the Nominal handover

logic and the new Hemispheric Handover (HH) logic, and the SRIF state error and uncertainties are documented at four points of interest in the orbit:

1. $\nu = 181°$, the data cutoff for OMM targeting,
2. $\nu = 202°$, 24 hours before perilune,
3. $\nu = 0°$, perilune itself, and
4. $\nu = 158°$, 24 hours after perilune.

In Table 3, the error statistics of the SRIF from each Monte Carlo analysis are detailed. There are four column pairs for average position error, average position uncertainty (1-σ), average velocity error, and average velocity uncertainty (1-σ). Each column pair lists the value for the nominal handover scheme and the hemispheric handover scheme. For every parameter except velocity uncertainty, the filter performance is improved by utilizing hemispheric handovers.

Table 3: Filter Performance with Nominal vs Hemispheric Handovers (HH) in a Crewed Scenario

ν	Position Error (km)		Position σ (km)		Velocity Error (cm/s)		Velocity σ (cm/s)	
	Nominal	HH	Nominal	HH	Nominal	HH	Nominal	HH
181	1.04	0.79	0.87	0.72	1.27	0.99	1.01	0.73
202	1.25	0.76	1.32	0.74	1.90	1.45	1.69	1.21
0	0.38	0.29	1.04	0.60	11.1	8.8	26.5	16.7
158	0.92	0.75	0.78	1.41	1.35	1.31	1.06	1.65

In Table 4, the percent reduction in error or uncertainty for each parameter at each point of interest is detailed. To be clear, a positive value is a reduction in error or uncertainty. Most parameters show a significant (double digit percent) reduction in error or uncertainty except a notable significant increase in velocity uncertainty at perilune +24h. This increased uncertainty is in opposition to the reduced error at the same point and warrants further investigation.

Table 4: Relative Reduction in Errors and Uncertainty between Nominal and Hemispheric Handover Schemes in a Crewed Scenario.

ν	Position Error	Position σ	Velocity Error	Velocity σ
181	23.8%	16.8%	22.0%	28.0%
202	39.4	43.9	23.7	28.4
0	25.0	42.5	20.7	37.0
158	17.9	-80.5	3.0	-55.7

It is also noted that the hemispheric handovers also accelerate the time frame for filter convergence for crewed scenarios. In Figure 6, the SRIF 1-σ uncertainty over time is plotted for the first half-revolution of the NRHO orbit for the Monte Carlo analysis with (a) the nominal handover scheme and (b) the hemispheric handover scheme. This shows the convergence of the filter from its initial state estimate and uncertainty, with some differences annotated in Figure 6 (b). The first annotation (a) highlights the significant reduction in position uncertainty when utilizing a hemispheric handover, and annotations (b) and (c) show repeated reductions in uncertainty
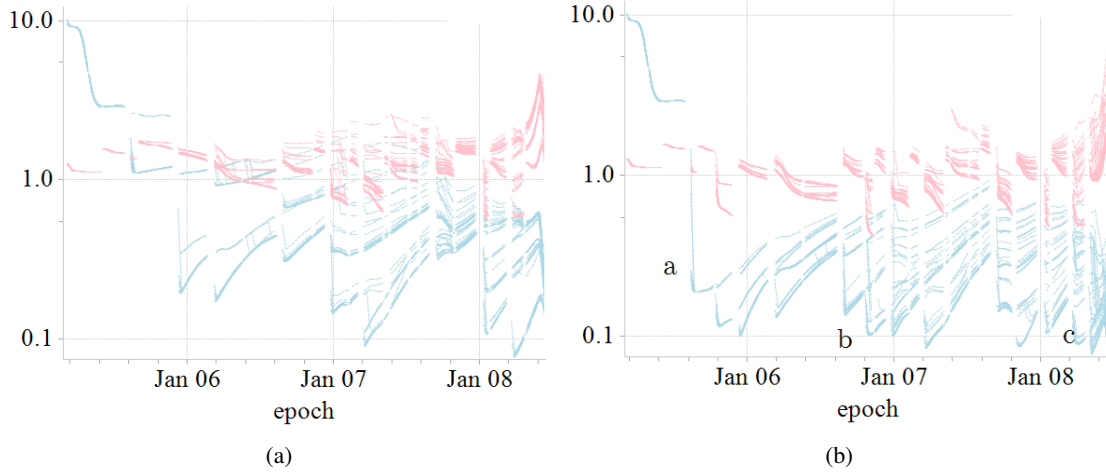
Figure 6: SRIF 1-σ uncertainty in position (blue) and velocity (red) for the first half-revolution with the (a) nominal handover scheme and (b) the hemisheric handover scheme for a crewed scenario.

OMM Reconstruction

The next analysis investigates the feasibility and performance of estimating OMM execution error through the repeated BLS invocations at perilune. As depicted in Figure 5, the BLS is executed at perilune of every revolution, and the OMM within the tracking data span is estimated within the BLS state vector. The simulation is then executed in an uncrewed scenario with three tracking data passes per revolution and thus in each BLS data span. To estimate OMM execution error, the Thrust Scale Factor (TSF) is estimated in the state vector.

To explore the design space of estimating TSF of OMMs in the BLS, four scenarios are each processed in a Monte Carlo analysis. To investigate the impact of DSN range bias on the observability of OMM TSF, the DSN range bias is turned off and on. Additionally, to investigate the optimal tuning for most accurately estimating OMM TSF, the initial uncertainty (i.e. the σ_0) on the TSF is adjusted between 1% and 5% of the OMM magnitude. The resulting reduction in TSF error appears in a box-whisker plot in Figure 7.

To recap for the unfamiliar: a box plot quickly displays statistical parameters in a way that a scatterplot obfuscates. The line inside the box is the mean, the box itself is the Interquartile Range (IQR, 50% of samples are in the box), the whiskers bound the Outer Quartile range (OQR, 99.3% of samples are within the whiskers), and remaining outliers are plotted individually. This plot shows the reduction in modeling error between a priori OMM estimate (initial estimated TSF = 1.0) and a posteriori OMM estimate. A positive value indicates a reduction in TSF error, e.g. a case that results in a 10% reduction means that the difference between the a priori TSF error and a posteriori TSF error is 10% of the OMM magnitude.

There are two main takeaways from this plot. First, the inclusion of DSN range biases decreases the performance of the BLS ability to estimate OMM TSF. This is shown as the reduction in mean and IQR of the error reduction in scenarios which modeled DSN range bias. Second, an initial uncertainty of 1% of the OMM magnitude performs slightly better than 5%. This is shown in the IQR and OQR bounds of the 1% case vs the 5% case.
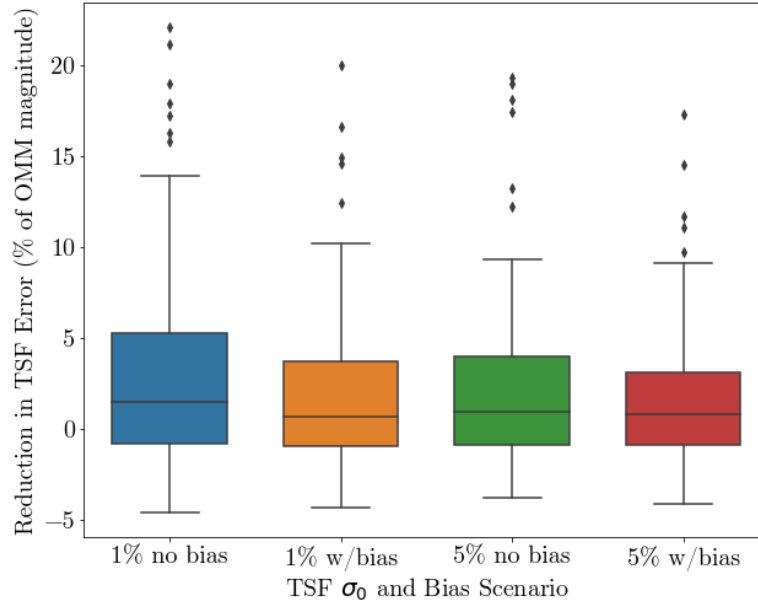
8

Figure 7: The reduction in TSF modeling error when estimated in post-processed BLS

The natural extension is to combine hemispheric handovers with OMM TSF estimation to investigate if the more variable tracking data geometry can allow better performance in estimating OMM TSF. Taking the "best" initial uncertainty parameters from the previous analysis, another Monte Carlo is executed with repeated BLS estimations of OMM TSF with an initial TSF uncertainty of 1.0%, this time utilizing tracking data simulated with the Hemispheric Handover scheme. In Figure 8, the reduction in TSF error statistics is shown for the nominal data scheme and the Hemispheric Handover scheme. The Nominal scheme plotted here is the same as the "1% w/ bias" case from Figure 7. OMM TSF estimation with BLS on tracking data that enforces Hemispheric Handovers has a higher mean reduction in error as compared to the nominal tracking data scheme.

Range Bias Estimation

The 2-way ranging data is subject to a range bias which is largely unobservable under typical filtering conditions in most of the NRHO away from perilune.[11] To more deeply investigate the performance of estimating range bias while in the NRHO, the BLS is employed to estimate range biases while considering each NRHO revolution as a unit. The first analysis estimates the range bias on each data pass while ignoring OMM execution error. That is, the BLS is not also estimating OMM TSF simultaneously. The simulation is run for a nine-revolution mission over 50 iterations. At three passes per revolution, a total of 1,350 tracking data passes are considered. In Figure 9, the accuracy of bias estimation per labeled pass appears in a box plot.
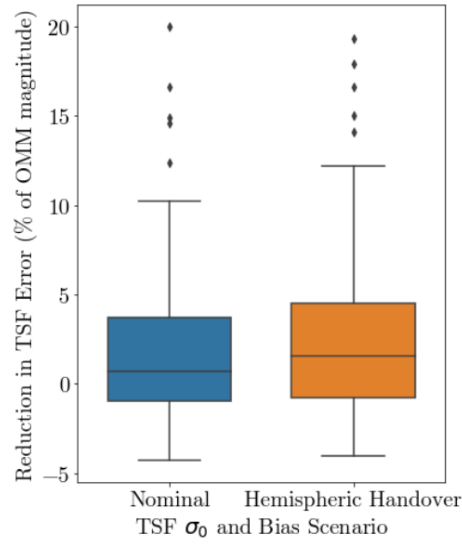
9

Figure 8: Reduction in TSF modeling error when estimated in post-processed BLS and with Hemispheric Handovers enforced in the tracking data.
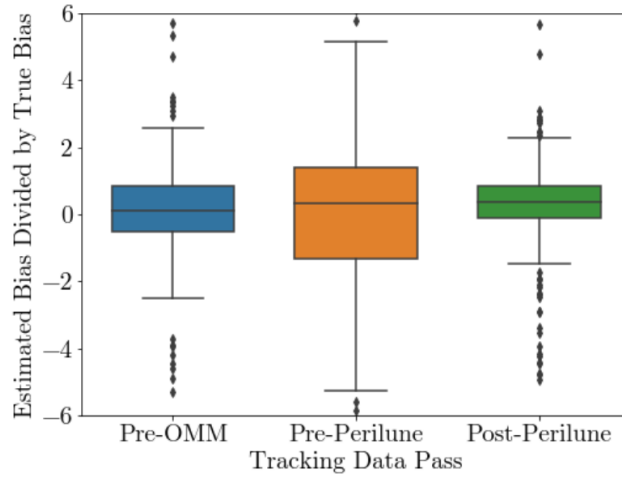

Figure 9: Estimated Bias Divided by True Bias for each Tracking Data Pass.

In Figure 9, the ratio of Estimated over True bias is plotted for each tracking data pass in a box-wing plot. A perfectly estimated bias returns a ratio of unity. Negative values suggest that the bias estimation in the opposite direction of the true bias. A range of 0.5-1.5 is indicative of a BLS that is estimating bias roughly in the correct direction and magnitude. Multiples above 2 suggest that the BLS is aliasing other error sources into bias and is too sensitive in that estimation channel.

The results in Figure 9 suggest a negligible ability for the BLS to accurately estimate range bias with this tracking scenario and BLS process. The mean being centered near zero for each tracking data pass suggests that the BLS is equally likely to estimate a bias in the wrong direction as in the correct direction. The wider variance in estimation error for the Pre-Perilune tracking data pass is an artifact of the BLS state estimate vector epoch being placed at the OMM epoch.

It has been found in simulation that range bias may be more observable in the immediate vicinity of Perilune, within approximately 4 hours before or after perilune.[11] To explore this possibility with the BLS, the pre- and post-perilune tracking data passes are moved to be immediately before and after perilune, respectively. The Monte Carlo analysis is then run to repeatedly execute the BLS to estimate tracking data bias with the adjusted tracking schedule. The bias estimation accuracy appears in a box plot in Figure 10.
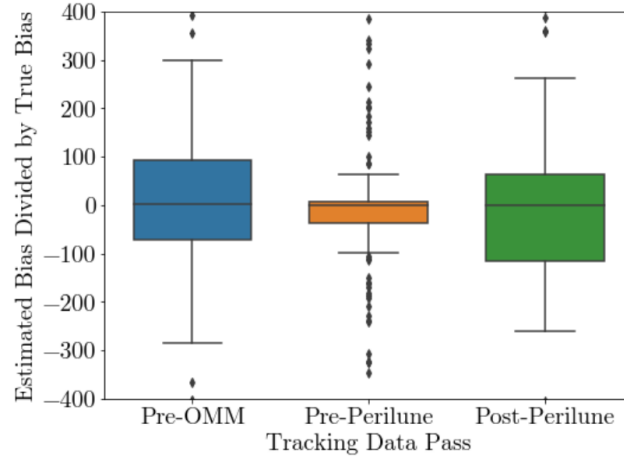

Figure 10: Estimated Bias Divided by True Bias for each Tracking Data Pass with Pre/Post Perilune Passes connecting over Perilune.

The BLS struggles with tracking data close to perilune. The astronomically large bias estimates seen in Figure 10 suggest that the BLS is responding to the dynamics of perilune by absorbing state error into the range bias. Adjusting the epoch of the state estimate solution away from pre-OMM made the residuals and estimation failed to improve bias estimation results. Particular care must be taken with individual tracking data passes when they are close to perilune.

While the performance of estimating range bias is marginal, it could be that estimated state solutions are more accurate when including biases in the estimated state vector. If estimated position and velocity state solutions are more accurate regardless of bias estimation performance, then including biases in the BLS process would still have value. In Figure 11, the state estimate solution error for each BLS processing scenario is shown in a box plot.

In Figure 11, the Baseline scenario ignores the effects of DSN range bias and OMM execution error, the "Est. Biases" scenario estimates range bias while ignoring OMM execution error, and the "Est. OMMs" scenario estimates OMM TSF while ignoring DSN range biases. The sensitivity of solution accuracy to these BLS considerations is minimal. The scenario in which the BLS is estimating OMM TSF shows the smallest variance in velocity estimation error, and also returns valuable TSF parameters, while the bias estimates from the "Est. Biases" scenario have been shown to not be accurate.

BLS Notes

A BLS capability will likely be an available tool for Gateway operations. Its ability to consider multiple passes and events together can introduce valuable capability in reconstructing OMMs. There are some notable drawbacks compared to filtering with respect to operational considerations.
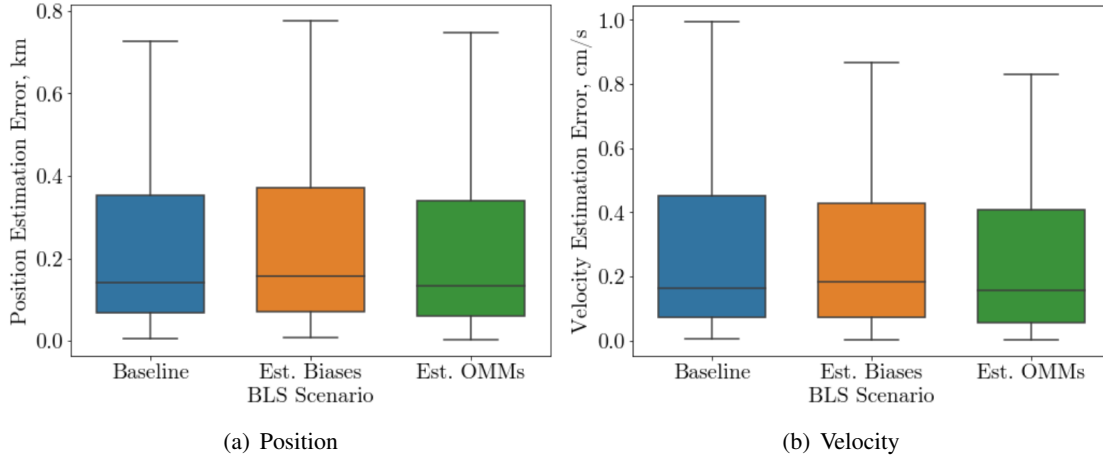
(a) Position   (b) Velocity

Figure 11: State Estimate Errors for BLS Scenarios in a) Position and b) Velocity.

The BLS struggles with tracking data near perilune and in operations would require manual intervention to adjust a priori bias and state values to guide the BLS towards a solution that makes physical sense in the context of NRHO operations.

Operations on crewed missions require the ability to inspect and troubleshoot any aspect of procedure in order to verify performance and accuracy. Anomalies in crewed operations can trigger root cause investigations that must be able to glean precisely the mechanism of unexpected behavior. An example root cause could be a slightly erroneous value of transponder delay being considered in the 2-way tracking data that is discovered through empirical testing and needs to be adjusted for operations. Filtering systems that utilize automation to abstract away from minutiae may lose the deep inspection ability to flexibly adjust arbitrary OD parameters with quick turnaround. Conversely, sensitive manual systems that require repeated human intervention is costly over time, introduces its own set of human-related risks, and can inhibit advances in OD processes to improve mission performance.

It is ideal then to have both (or multiple) options for operations: an automated filtering system that is generally trustworthy and quickly responds to new tracking data and a manual, deep inspection OD tool that allows minute adjustment of any OD processing parameter, but requires intervention and analysis to produce a high quality state estimate solution. There is legacy behind the operations concept of having multiple navigation processes employed on a single data stream for a single mission, it is an approach typically employed by missions controlled out of the Jet Propulsion Laboratory (JPL).[14]

SUMMARY AND FORWARD WORK

The general motif of these analyses to adjust how 2-way tracking data is taken and processed in order to improve navigation performance without considering new data types such as deep space GPS, optical navigation, or X-Nav. A number of analyses that adjust the tracking schedule or process the tracking data in different configurations are performed to attempt to improve observation of the estimated state. Additional partner sites with advantageous geometry and a tracking schedule that switches between north and south hemispheres for sequential tracking data passes is implemented and tested. It is shown that a hemispheric switching in tracking data scheduling can improve navigation solution accuracy and covariance performance.

To augment the nominal navigation filtering process, a BLS process is implemented to be executed at every perilune crossing and including the tracking data collected since the previous perilune crossing, as depicted in Figure 5. The BLS considers tracking data arcs, events, and the solution vector together in a batch vs sequentially which can offer the ability to reconstruct maneuvers and estimate tracking data range biases. The BLS shows promise in estimating OMM execution error in the form of a thrust scale factor (see Figure 7), and this performance is improved with hemispheric handovers (see Figure 9). However, this success does not extend to estimating tracking data range bias. Several approaches to estimating range bias with the BLS are explored, with marginal success. Further analysis into best practices of utilizing the BLS is warranted, as well as including a radiometric ground tracking data type such as 3-way downlinked data with partner sites.

These analyses can be extended further into the crewed scenarios, and can include detection of perturbations. The feasibility, performance, and the optimal batching of continuous data for the BLS on a crewed scenario can be investigated. More generally, the development and analysis of a suite of OD processing tools for navigation in the NRHO can produce value in guiding the requirements of operational systems. Lessons learned in development and execution of simulated tools can be applied to the development of operational tools to prepare for operations in a novel regime of trajectories.

ACKNOWLEDGEMENTS

REFERENCES

[1] W. H. Gerstenmaier, "Progress in Defining the Deep Space Gateway and Transport Plan," https://www.nasa.gov/sites/default/files/atoms/files/nss_chart_v23.pdf, Mar. 28, 2017.

[2] R. Whitley and R. Martinez, "Options for Staging Orbits in Cis-Lunar Space," *2016 IEEE Aerospace Conference*, 2016.

[3] E. W. Kayser, J. S. Parker, M. J. Bollinger, T. Gardner, and B. W. Cheetham, "The Cislunar Autonomous Positioning System Technology Operations and Navigation Experiment," 2020.

[4] C. P. Newman, D. C. Davis, R. J. Whitley, J. R. Guinn, and M. S. Ryne, "Stationkeeping, Orbit Determination, and Attitude Control for Spacecraft in Near Rectilinear Halo Orbits," *Paper No. AAS 18-388, AAS Astrodynamics Specialist Conference, Snowbird, Utah*, August 2018.

[5] M. J. Volle and D. C. Davis, "Examining the Ferasibility of Relative-Only Navigation for Crewed Missions to Near Rectilinear Halo Orbits," *AAS/AIAA Astrodynamics Specialists Conference*, Snowbird, Utah, August 2018.

[6] M. J. Volle, "Distant retrograde Orbit Constellations for Relative-Only Navigation in Near Rectilinear Halo Orbits," *AAS/AISS Spaceflight Mechanics Meeting*, Ka'anapali, Hawaii, January 2019.

[7] L. B. Winternitz, W. A. Bamford, A. C. Long, and M. Hassouneh, "GPS Based Autonomous Navigation Study for the Lunar Gateway," *AAS Guidance, Navigation, and Control Conference*, Breckenridge, Colorado, February 2020.

[8] N. Parrish, M. J. Bollinger, E. W. Kayser, M. R. Thompson, J. S. Parker, B. W. Cheetham, D. C. Davis, and D. J. Sweeney, "Near Rectilinear Halo Orbit Determination with Simulated DSN Observations.," *AIAA Scitech 2020 Forum*, Orlando, Florida, March 2020.

[9] M. J. Bollinger, M. R. Thompson, N. P. Ré, C. Ott, and D. C. Davis, "Ground-Based Navigation Trades for Operations in Gateway's Near Rectilinear Halo Orbit," *AAS/AIAA Astrodynamics Specialist Conference*, Big Sky, Virtual, August 2021.

[10] C. P. Newman, R. Sieling, D. C. Davis, and R. J. Whitley, "Attitude Control and Orbit Determination of a Crewed Spacecraft with Lunar Lander in Near Rectilinear Halo Orbit," *29th AAS/AIAA Space Flight Mechanics Meeting*, Ka'anapali, Hawaii, February 2019.

[11] C. Ott, M. Bollinger, M. Thompson, and N. P. Re, "Range Biases, Measurement Noise, and Perilune Accuracy in Near Rectilinear Halo Orbit Navigation," *AIAA Scitech Forum and Exposition*, San Diego, California, January 2022.

[12] D. C. Davis, S. A. Bhatt, K. C. Howell, J. Jang, R. L. Whitley, F. D. Clark, D. Guzzetti, E. M. Zimovan, and G. H. Barton, "Orbit Maintenance and Navigation of Human Spacecraft at Cislunar Near Rectilinear Halo Orbits," *27th AAS/AIAA Space Flight Mechanics Meeting*, San Antonio, Texas, February 2017.

[13] D. E. Lee, "White Paper: Gateway Destination Orbit Model: A Continuous 15 Year NRHO Reference Trajectory," Tech. Rep. Document ID: 20190030294, National Aeronautics and Space Administration, NASA Johnson Space Center, Houston, TX, August 2019.

[14] T. You, A. Halsell, D. Highsmith, M. Jah, S. Demcak, E. Higa, S. Long, and S. Bhaskaran, "Mars Reconnaissance Orbiter Navigation," *AIAA/AAS Astrodynamics Specialists Conference and Exhibit*, Providence, Rhode Island, August 2004.